Review

J. Astrophys. Astr., Vol. 36, No. 4, December 2015, pp. 581–588

Modeling of Stark–Zeeman Lines in Magnetized Hydrogen Plasmas

J. Rosato*, H. Bufferand, H. Capes, M. Koubiti, L. Godbert-Mouret, Y. Marandet & R. Stamm

Aix-Marseille Université, CNRS, PIIM UMR 7345, F-13397 Marseille Cedex 20, France.
**e-mail: joel.rosato@univ-amu.fr*

Received 12 June 2015; accepted 7 September 2015
DOI: 10.1007/s12036-015-9353-x

Abstract. The action of electric and magnetic fields on atomic species results in a perturbation of the energy level structure, which alters the shape of spectral lines. In this work, we present the Zeeman–Stark line shape simulation method and perform new calculations of hydrogen Lyman and Balmer lines, in the framework of magnetic fusion research. The role of the Zeeman effect, fine structure and the plasma's non-homogeneity along the line-of-sight are investigated. Under specific conditions, our results are applicable to DA white dwarf atmospheres.

Key words. Line shapes—plasma diagnostic—Stark broadening—Zeeman effect.

1. Introduction

The plasma at the edge of magnetic fusion devices (tokamaks or stellarators) presents features similar to the atmospheres of A-type white dwarfs: it is mainly composed of hydrogen (and isotopes), the temperatures are relatively low (∼1–10 eV), the electron density ranges from 10^{12} to 10^{15} cm^{-3}, and a strong magnetic field (up to several teslas) is present. By analogy with astrophysics, spectroscopy is used as a diagnostic tool and specific models and codes are used for the interpretation of spectral line shapes and intensities (Dimitrijevic *et al.* 2011). In this work, we report on the current status in hydrogen line shape modeling involving Stark and Zeeman effects for Lyman and Balmer lines with a 'moderate' principal quantum number, typically lower than 20. A specific issue that requires careful consideration is the role of the evolution of the microscopic electric field at the time scale relevant to the line formation (time-of-interest), which is of the order of the inverse line width. After a presentation of the line broadening formalism, we report on calculations of line shapes using a simulation method developed for magnetic fusion plasma diagnostics (Rosato *et al.* 2009). As in astrophysics, magnetic fusion plasmas may be subject to line radiation trapping and accurate line shape models are involved in radiation transport codes. In this context, we also present calculations of Doppler-free

line shapes and discuss the sensitivity of fine structure lines to the magnetic field. An investigation of the role of the plasma's non-homogeneity along the line-of-sight on an observed spectrum is also reported.

2. Line shape theory

We give a brief overview of the formalism used in line shape modeling, along the lines of standard textbooks (e.g. Griem 1974) and following some of our previous works, e.g. Rosato *et al.* (2014). We denote $I(\omega, \mathbf{n})$, the intensity of a spectral line emitted at the angular frequency ω and in the direction $\mathbf{n}$. This quantity is given in terms of the line profile in the atom's frame of reference $I_0(\omega, \mathbf{n})$ by Doppler convolution

$$I(\omega, \mathbf{n}) = \int \mathrm{d}^3 v f(\mathbf{v}) I_0(\omega - \omega_0 \mathbf{v} \cdot \mathbf{n}/c, \mathbf{n}). \tag{1}$$

Here, ω_0 is the central frequency of the line under consideration and $f(\mathbf{v})$ is the atoms' velocity distribution (VDF). For Maxwellian VDF, the line shape is a Gaussian function if there is no broadening mechanism in the atom's frame of reference (i.e. when $I_0(\omega, \mathbf{n}) \equiv \delta(\omega - \omega_0)$) and a Voigt function if natural broadening is retained. In the general case, $I_0(\omega, \mathbf{n})$ is proportional to the Fourier transform of the atomic dipole autocorrelation function $C_{\mathbf{n}}(t)$, a quantity described in the framework of quantum mechanics

$$I_0(\omega, \mathbf{n}) = \frac{1}{\pi} \mathrm{Re} \int_0^\infty \mathrm{d}t C_{\mathbf{n}}(t) \mathrm{e}^{i\omega t}, \tag{2}$$

$$C_n(t) = \sum_{\alpha\alpha'\beta\beta'\varepsilon} \rho_{\alpha\alpha} (\mathbf{d}_{\alpha\beta} \cdot \varepsilon)(\mathbf{d}^*_{\alpha'\beta'} \cdot \varepsilon) \{U_{\alpha'\alpha}(t) U^*_{\beta'\beta}(t)\}. \tag{3}$$

Here, ρ is the restriction of the density operator to the atom's Hilbert space evaluated at initial time, $\mathbf{d} \cdot \varepsilon$ is the dipole projected onto the polarization vector ε (perpendicular to $\mathbf{n}$), the indices α, α' (resp. β, β') are used for matrix elements and denote states in the upper (resp. lower) level, the brackets $\{\ldots\}$ denote an average over the perturber trajectories, and $U(t)$ is the evolution operator. It obeys the time-dependent Schrödinger equation

$$i\hbar \frac{\mathrm{d}U}{\mathrm{d}t}(t) = [H_0 + V(t)]\, U(t). \tag{4}$$

Here H_0 is the Hamiltonian including both the atomic energy level structure (with a non-Hermitian part accounting for natural broadening) and the Zeeman effect, and $V(t) = -\mathbf{d} \cdot \mathbf{F}(t)$ is the time-dependent Stark effect term (Schrödinger picture) resulting from the action of the microscopic electric field $\mathbf{F}(t)$. When this term is neglected, the Schrödinger equation has the trivial solution $U(t) = \exp(-iH_0 t/\hbar)$, which shows, using equations (3) and (2), that $I_0(\omega, \mathbf{n})$ reduces to a set of delta functions (or Lorentzian functions if the natural broadening is retained). By contrast, the case where $\mathbf{F}(t)$ is significant is much trickier because there is no general exact analytical solution. The time-dependent perturbation theory yields a formal expansion (Dyson series), which is not applicable in explicit calculations because of the non-commutation of the interaction term at different times (time-ordering problem). This

concerns, in particular, the microfield due to ions. Several models, based on suitable approximations, have been developed in such a way as to provide an analytical expression for the line shape (e.g., the impact and static approximations, the model microfield method, etc.). For our purposes, it is convenient to have a line shape model that is free from such approximations, in such a way as to make it applicable to various plasma conditions. A good candidate is the so-called simulation technique (Stamm & Voslamber 1979; Stambulchik & Maron 2010).

3. Line broadening mechanisms

We discuss here the line broadening mechanisms in tokamak edge plasma conditions. Profiles of Lyman and Balmer lines with a low upper principal quantum number n have been calculated using the simulation method. In the plasma microfield Stark broadening model, the ions are described as particles moving along straight lines around the emitter, in a cube with periodic boundary conditions; the initial conditions (on the positions and velocities of the perturbers) are generated randomly; correlations are retained through the use of a Debye electric field model; and the broadening due to the electrons is described with a collision operator (e.g., see Rosato *et al.* 2009 for details on the code). The Zeeman effect and the fine structure are retained through their corresponding Hamiltonians. The average over the atom's velocities (equation (1)), required for the Doppler broadening, is formed by random sampling using a Maxwellian VDF. Figure 1 gives an illustration of the relative importance of the Stark effect with respect to the Doppler broadening on the Hα line, at conditions relevant to tokamak divertor plasmas in the recombining regime (Lipschultz *et al.* 1998). This line is routinely observed in tokamak edge plasmas and it can provide information on the atomic VDF (from Doppler broadening). The spectrum has been calculated here assuming a high value (10^{15} cm^{-3}) for the electron density, which can be attained in specific discharge scenarios. The Stark width is of the same order as the Doppler width, indicating that it should be retained in a fitting routine for

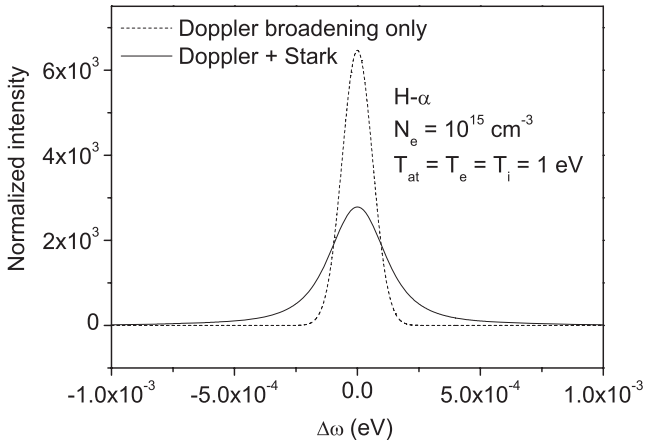

Figure 1. Plot of the hydrogen Balmer α line shape in high-density tokamak divertor plasma conditions. The line shape is about twice larger when Stark broadening is retained.

diagnostics. The presence of a strong magnetic field (not retained in Figure 1) also requires careful considerations in the establishment of a Stark broadening model. The Zeeman effect alters the energy level structure, which affects the strength of the Stark perturbation. The degeneracy removal can result in a reduction of the width of the Zeeman Lorentz triplet lateral components, which should be retained in a diagnostic routine if accuracy is required (see Figure 2) (Rosato *et al.* 2009, 2012a). The fine structure is usually not visible on hydrogen lines in magnetic fusion plasma conditions (due to strong Doppler broadening) but its role can be significant in the photon–atom interaction processes involved in Lyman radiation transport, because it can be comparable to the Zeeman effect in the atomic frame of reference. Recent investigations of Lyman radiation trapping in optically thick divertor conditions have prompted an interest in the establishment of analytical line shape models accounting simultaneously for the Zeeman effect and the fine structure (Rosato *et al*. 2010a). Figure 3 shows an example of the line shape calculated retaining fine structure in the atomic frame of reference. We have chosen a set of conditions relevant to an experiment of saturation spectroscopy reported in (Asakawa *et al.* 2012). Doppler-free spectra of Hα were observed in the presence of a magnetic field of 350 G. The electron density is small here (10^{11} cm^{-3}) and the line width is mainly due to natural broadening. As can be seen, the spectrum is strongly dependent on the magnetic field, and there is no simple relation between the intensity and the positions of the components and the magnetic field strength. The simulation method (as well as any line shape code) is able to reproduce the position of the line components, provided a correct atomic database is used. It is worth noting that the energy shift due to the interactions between the atom and the 'vacuum' field (Lamb effect) is comparable to the other energy level splitting mechanisms and should be retained here (see Fig. 4).

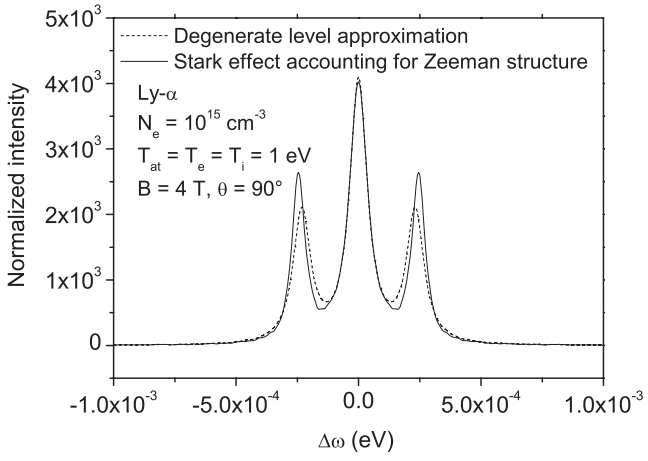

Figure 2. The 'accidental' degeneracy of the hydrogen energy levels is partially removed when a magnetic field is present, which alters the strength of the Stark perturbation. Here, this is illustrated on the Lyman α Lorentz triplet. For the sake of clarity, Doppler broadening has not been retained. The dashed (respectively solid) line corresponds to a calculation of Stark broadening that neglects (respectively retains) the Zeeman degeneracy removal. The degeneracy removal results in a reduction of the width of the lateral components. A slight shift is also present.

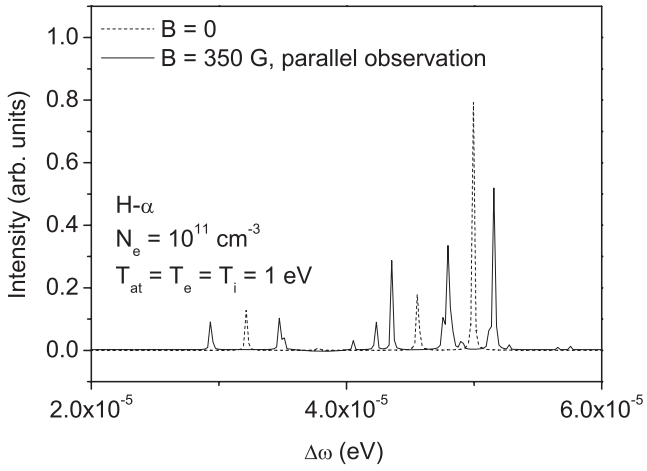

Figure 3. Plot of the Hα line shape calculated in conditions of a plasma experiment involving saturation spectroscopy techniques (Asakawa *et al.* 2012). When Doppler broadening is eliminated, the line exhibits fine structure components, whose position and relative intensities depend on the magnetic field strength in a not straightforward fashion. The magnetic field value of 350 G corresponds to that set in Asakawa *et al.* (2012).

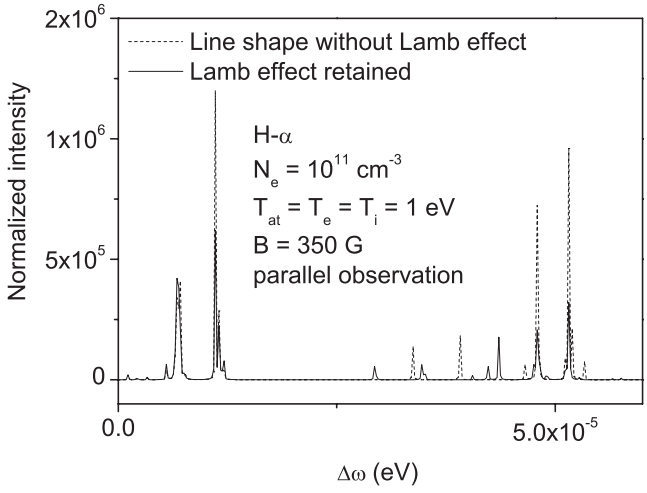

Figure 4. Plot of the Doppler-free Hα line shape at the same conditions as in Figure 3. The interaction between the 'vacuum' electromagnetic field (Lamb effect) is comparable to other broadening mechanisms, indicating that this effect should be retained in spectrum analysis.

4. Analysis of synthetic spectra

In the previous section, it has been shown that a reliable interpretation of hydrogenic spectral line shapes for diagnostics in tokamak edge and divertor plasmas should involve the use of accurate line broadening models. An additional problem that occurs in applications is the non-uniformity of the emission zone along the line-of-sight. The formation of a spectral line results from the emission of atoms that are

located in regions with different values of N_e, T_e, etc., which renders the interpretation of spectra intricate. In recent years, modeling efforts have been carried out with the purpose of analyzing spectrum signals observed in a virtual plasma background obtained from a transport code (synthetic diagnostics, e.g. Rosato *et al.*, 2012b, 2015). As an illustration, we show here, an example of application to the Dα line observed in a virtual plasma background calculated from the SolEdge2D-EIRENE code (Bufferand *et al.* 2015). Relevant values obtained for the divertor region include an electron density of the order of 10^{14} cm^{-3} (see Fig. 5), temperatures of several electron-volts (Fig. 6), and a magnetic field of about 4.4 T. Given a line-of-sight crossing this plasma background, the following integral has been calculated:

$$\int_0^L \mathrm{d}s N_3(s) I(\omega, s). \tag{5}$$

Here, L is the length of the line-of-sight and s is a curvilinear coordinate that parametrizes the space dependence of the emission profile I (frequency normalized line shape) along the line-of-sight. This dependence is implicit through the plasma parameters N_e, T_e, etc. The quantity N_3 denotes the density of atoms present in the excited state ($n = 3$); it also depends on the space through the plasma parameters. We have evaluated this quantity from the same collisional-radiative model as in Rosato *et al*. (2010a, b) (the coronal limit is not systematically attained, e.g. Fujimoto 2004). Note that the propagation vector **n** is a constant and has not been written here for the sake of simplicity. The local emission profile at each location on the line-of-sight has been evaluated from the line shape simulation method presented in the previous section. Figure 7 shows the obtained profile of Dα, together with the result of an adjustment with a three-Gaussian line shape model accounting for the Zeeman and Doppler effects. The adjustment routine (already used in Rosato *et al*. (2010b))

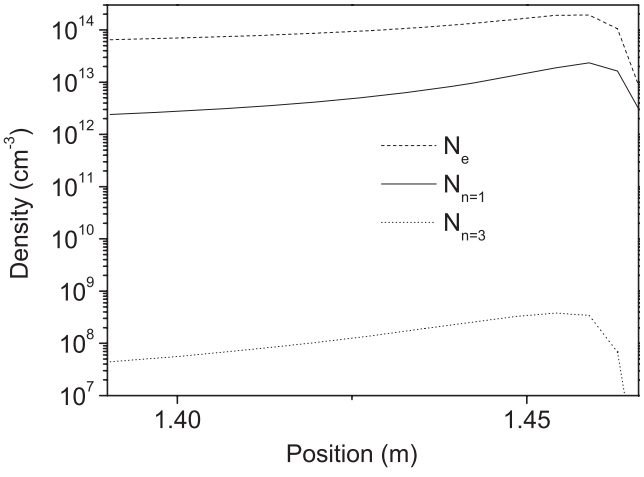

Figure 5. Plot of the density of electrons and atoms in the ground state ($n = 1$), obtained from a transport code, along a line-of-sight crossing the divertor of the WEST tokamak, an upgrade of Tore Supra currently under construction in Cadarache (France). Also shown in the figure is the density of atoms in the excited state ($n = 3$) calculated using a collisional-radiative model (Rosato *et al*. (2010a, b).

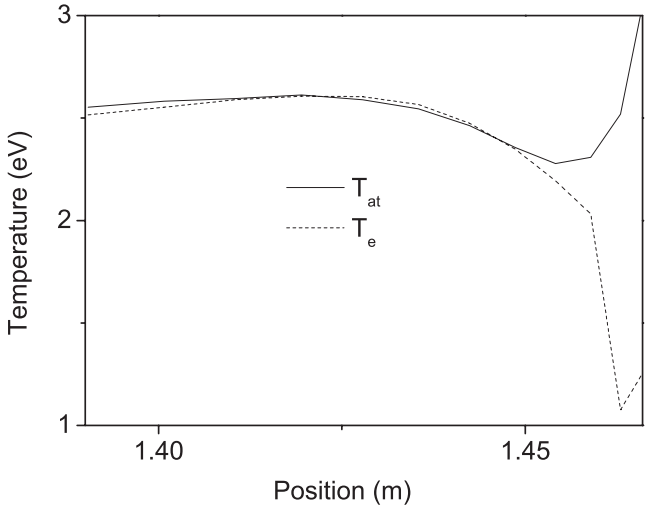

Figure 6. Plot of the electronic and atomic temperatures calculated along the same line-of-sight as in Figure 5. Typical values in the divertor are of the order of several electron-volts.

performs a χ^2 minimization and is based on a genetic algorithm method (PIKAIA code; the routine, together with examples of use in astrophysics, are available in Charbonneau (1995)). The routine evaluates the set of optimal parameters ($T_{\rm at}$, B, θ) that minimizes the distance between the frequency normalized simulated spectrum (i.e., resulting from line-of-sight integration according to equation (5)) and the three-Gaussian model. Our application to the Dα line profile yields an atomic temperature of 3.1 eV, which provides a correct order of magnitude. The obtained values for the magnetic field and the angle of observation θ correspond to those at the densest

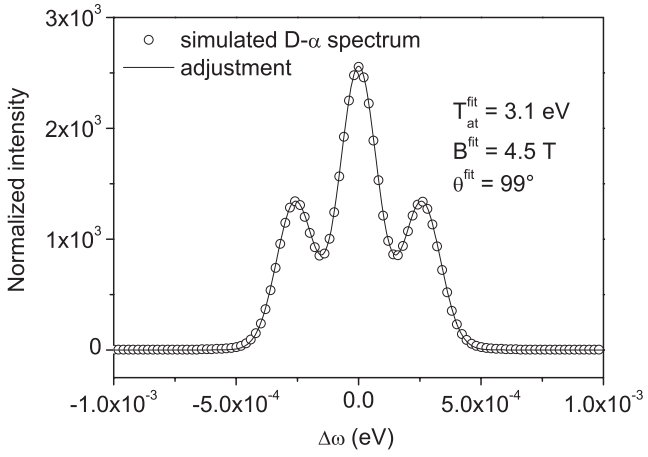

Figure 7. Plot of the apparent profile of Dα, as it would result from a passive observation in the WEST divertor plasma. An adjustment using a Zeeman–Doppler line shape model provides the correct order of magnitude for the atomic temperature.

location within 10%. Note that the atomic temperature at the densest location on the line-of-sight is significantly lower (2.3 eV) than the value extracted from the fitting routine; this deviation can be due to a misinterpretation of the spectrum owing to the neglect of Stark broadening in the model. A possible extension of the fitting model could retain this effect with an analytical formula, e.g., using a frequency-dependent collision operator model (Rosato *et al*. 2012b).

5. Conclusion

As in astrophysics, passive spectroscopy of atomic line radiation is used for the diagnostic of magnetic fusion plasmas. In this context, we have presented the state-of-art in line shape modeling techniques, with a special emphasis on their applicability to tokamak edge plasmas in the context of ITER operation. In general, the magnetic field is sufficiently strong so that hydrogen lines with a low upper principal quantum number are affected by the Zeeman effect. In this framework, we have shown that the line broadening due to the Stark effect is sensitive to the Zeeman energy level structure, suggesting the importance of retaining these effects simultaneously in a model. We have also shown that the Zeeman effect may result in a complex structure if the field is weak; this structure can be observed and investigated using saturation spectroscopy techniques that involve Doppler-free line profiles. The possibility of extracting local information on the plasma parameters from passive spectroscopy has been illustrated from synthetic spectra analysis involving a virtual plasma background. Such an analysis could also be performed in astrophysics, e.g. on absorption lines observed in stellar atmospheres.

Acknowledgements

The authors would like to acknowledge the financial support from the Agence Nationale de la Recherche, project ANR-11-BS09-023 (SEDIBA).

References

Asakawa, R. *et al.* 2012, *JINST*, **7**, C01018.
Bufferand, H. *et al.* 2015, *Nucl. Fusion*, **55**, 053025.
Charbonneau, P. 1995, *Astrophys. J. Suppl. Ser.*, **101**, 309.
Dimitrijevic, M. S. *et al.* 2011, *Balt. Astron.*, **20**, 495.
Fujimoto, T. 2004, *Plasma Spectroscopy* Clarendon Press, Oxford.
Griem, H. R. 1974, *Spectral Line Broadening by Plasmas* Academic Press, London.
Lipschultz, B. *et al.* 1998, *Phys. Rev. Lett.*, **81**, 1007.
Rosato, J. *et al.* 2009, *Phys. Rev. E*, **79**, 046408.
Rosato, J. *et al.* 2010a, *Contrib. Plasma Phys.*, **50**, 398.
Rosato, J., Kotov, V., Reiter, D. 2010b, *J. Phys. B: At. Mol. Opt. Phys.*, **43**, 144024.
Rosato, J. *et al.* 2012a, *J. Phys. B: At. Mol. Opt. Phys.*, **45**, 165701.
Rosato, J., Capes, H., Stamm, R. 2012b, *Phys. Rev. E*, **86**, 046407.
Rosato, J., Marandet, Y., Stamm, R. 2014, *J. Phys. B: At. Mol. Opt. Phys.*, **47**, 105702.
Rosato, J. *et al.* 2015, *J. Quant. Spectrosc. Radiat. Transfer*, **165**, 102.
Stamm, R., Voslamber, D. 1979, *J. Quant. Spectrosc. Radiat. Transfer*, **22**, 599.
Stambulchik, E., Maron, Y. 2010, *High Energy Density Phys.*, **6**, 9.